Closed-form minimax time-delay filters for underdamped systems

Tarunraj Singh[1,*,†] and Marco Muenchhof[2]

[1] *Department of Mechanical and Aerospace Engineering, SUNY at Buffalo, Buffalo, NY 14260, U.S.A.*
[2] *Institute for Automatic Control, TU Darmstadt, Darmstadt, Germany*

SUMMARY

This paper derives closed-form solutions for the parameters of a time-delay filter designed to be robust to uncertainties in frequencies to be cancelled. It is shown that the slope of the magnitude plot of the two time-delay filter is zero at the nominal frequency indicating that it is a local maximum. This information is used for deriving the solution of the parameters of the time-delay filter in closed form. Three time-delay filters are also designed which force a zero of the filter to be located at the nominal frequency of the system. Uniform and non-uniform distributions of the penalty over the uncertain regions are permitted in this formulation. The applicability of the proposed technique for the control of multi-mode systems is also illustrated. Copyright © 2006 John Wiley & Sons, Ltd.

1. INTRODUCTION

Vibration attenuation by shaping input to underdamped systems has been addressed by numerous researchers [1–6] besides others. There has been an increased interest in the development of techniques to desensitize the controllers to uncertainties in the system model. The requirements of high precision in applications such as hard disk drives [7], telescopes [8, 9], etc. mandate that the controllers satisfy the pointing requirements in the presence of uncertainties in the model. Singer and Seering [2] proposed a technique to design a sequence of impulses with the objective of forcing the variation of the sensitivity of the residual energy of the system with respect to modelled damping or frequency to zero. The resulting controllers

---

*Correspondence to: Tarunraj Singh, Department of Mechanical and Aerospace Engineering, SUNY at Buffalo, Buffalo, NY 14260, U.S.A.
†E-mail: tsingh@eng.buffalo.edu

were called *input shapers*. Singh and Vadali [5] illustrated that robustness to modelling errors can be achieved by cascading multiple time-delay filters designed to cancel the nominal poles of the system. Singhose *et al.* [10] proposed a technique which they referred to as multi-hump extra-insensitive (EI) input shaper where they determine the amplitudes of the impulses so as to maximize the uncertain domain where the residual vibration is below a specified threshold. Singh [11] proposed an optimization problem where the maximum magnitude of the residual energy in an uncertain domain is minimized. The difference between the EI input shaper and the minimax time-delay filter is that the EI shaper requires the residual energy curve to be zero at two frequencies which flank the nominal frequency of the considered mode. However, this constraint is not required in the minimax formulation and minimax design results in a larger uncertainty domain for any specified residual energy threshold, which corresponds to increased robustness. Singhose *et al.* [12] also illustrate the benefit of using the input shaping technique (time-delay filter) compared to conventional Finite Impulse Response (FIR) and Infinite Impulse Response (IIR) filters. In this paper, the minimax problem is first addressed for a single mode system. In numerous applications, there exists one dominant mode which is the main contributor to the residual energy of the manoeuvring structure. Thus, there is a motivation to derive the optimal time-delay filter which minimizes the maximum magnitude of the transfer function of the time-delay filter, in closed form. A simple technique for handling multiple modes is also proposed. The resulting filter is designed by addressing the problem as a series of single mode problems.

Section 2 focuses on the development of closed-form solutions for the parameters of minimax time-delay filters. The development is then modified to permit differential weighting of the limiting and nominal frequencies. In Section 3, a simple approach is proposed to permit using the solution of the undamped systems to system with damping. The approach to design minimax filters for multi-mode systems is described in Section 4. The paper concludes with some remarks in the final section.

2. OPTIMAL MINIMAX FILTERS FOR UNDAMPED SYSTEMS

2.1. Two time-delay filter

A time-delay filter to modify the reference input to a system to attenuate residual vibrations is shown in Figure 1.

The transfer function of the time-delay filter is given by the equation

$$A_0 + A_1 \, \mathrm{e}^{-sT_1} + A_2 \, \mathrm{e}^{-sT_2} \tag{1}$$

which is used to prefilter inputs to a system characterized by undamped modes. The frequency of the mode to be cancelled is uncertain, but the region of uncertainty is known. Assume that the nominal frequency is ω_0 and the uncertain frequency ω lies in the range

$$\omega_l \leqslant \omega \leqslant 2\omega_0 - \omega_l \tag{2}$$

implying that the uncertainty is symmetric about the nominal frequency. Figure 2 illustrates schematically the objective of the optimization problem where the maximum magnitude of the cost function over the domain of uncertainty ω_l to $2\omega_0 - \omega_l$ is to be minimized. To minimize the maximum magnitude of the magnitude plot of the time-delay filter in the region of uncertainty

$$\xrightarrow{r(s)} \boxed{A_0 + A_1 e^{-sT_1} + A_2 e^{-sT_2}} \longrightarrow \boxed{\frac{\omega^2}{s^2+\omega^2}} \xrightarrow{y(s)}$$
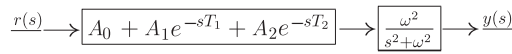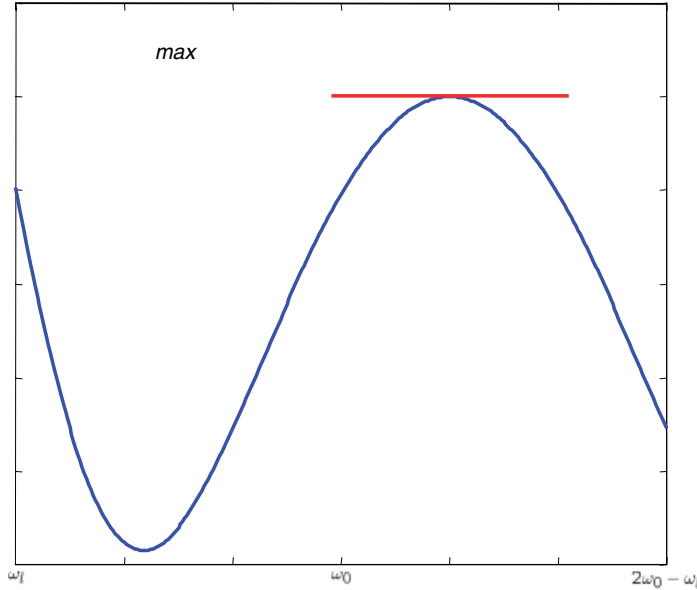
Figure 1. Time-delay filter.

Figure 2. Sensitivity curve.

(Figure 2), we require that the magnitude of the time-delay filter at the boundary be equal to that at the nominal frequency. Assuming further that

$$T_1 = \frac{\pi}{\omega_0} \quad \text{and} \quad T_2 = \frac{2\pi}{\omega_0} \tag{3}$$

the magnitude of the transfer function of the time-delay filter can be shown to be

$$F(\omega) = A_0^2 + A_1^2 + A_2^2 + 2A_0A_1 \cos\left(\frac{\omega}{\omega_0}\pi\right) + 2A_0A_2 \cos\left(\frac{2\omega}{\omega_0}\pi\right) + 2A_1A_2 \cos\left(\frac{\omega}{\omega_0}\pi\right) \tag{4}$$

The location of the maximum of $F(\omega)$ can be determined from the equation

$$\frac{\mathrm{d}F(\omega)}{\mathrm{d}\omega} = -2A_0A_1 \frac{\pi}{\omega_0}\sin\left(\frac{\omega}{\omega_0}\pi\right) - 2A_0A_2 \frac{2\pi}{\omega_0}\sin\left(\frac{2\omega}{\omega_0}\pi\right) - 2A_1A_2 \frac{\pi}{\omega_0}\sin\left(\frac{\omega}{\omega_0}\pi\right) = 0 \tag{5}$$

It can be seen that $\omega = \omega_0$ satisfies Equation (5). To determine the parameters of the minimax time-delay filter, the magnitude of the time-delay filter at the boundary and the nominal frequency are equated, resulting in the equation

$$\left(A_0 + A_1 \cos\left(\frac{\omega_l}{\omega_0}\pi\right) + A_2 \cos\left(\frac{2\omega_l}{\omega_0}\pi\right)\right)^2 + \left(A_1 \sin\left(\frac{\omega_l}{\omega_0}\pi\right) + A_2 \sin\left(\frac{2\omega_l}{\omega_0}\pi\right)\right)^2$$

$$= (A_0 + A_1 \cos(\pi) + A_2 \cos(2\pi))^2 \tag{6}$$

For undamped systems, we can assume that A_2 is equal to A_0. We also require the constraint

$$A_0 + A_1 + A_2 = 1 \tag{7}$$

to be satisfied to enable passing DC signals without amplification or attenuation. Solving for A_0, we have

$$A_0 = \frac{2(1 + \cos((\omega_l/\omega_0)\pi))}{5 + 4\cos((\omega_l/\omega_0)\pi) - \cos((2\omega_l/\omega_0)\pi)} \tag{8}$$

Figure 3 illustrates the variation of the gains of the time-delay filter as a function of the normalized uncertain interval. It can be seen that the amplitudes are always positive which is due to the fact that the delay time of the filter has been selected to be an integral multiple of half the period of the frequency to be cancelled. In the limit when ω_l/ω_0 equals unity, the optimal solution boils down to the robust time-delay filter designed to place two zeros at the estimated location of the poles of the system.

Calculating the magnitude of the time-delay filter at $\omega = 2\omega_0 - \omega_l$ using the solution for A_0 given by Equation (8), we can show that it is equal to that at the nominal frequency ω_0. Thus, the magnitude of the time-delay filter at the two limits of the uncertain frequency range and the nominal frequency are the same.

Figure 4 illustrates the variation of the magnitude of the transfer function of the time-delay filter which is referred to as the sensitivity curve, for different uncertain regions. It is clear from the figure that as the uncertain region decreases, the maximum magnitude of the sensitivity curve becomes smaller.

Since, the magnitude of the sensitivity plot at the nominal frequency is

$$(A_0 + A_1 \cos(\pi) + A_2 \cos(2\pi)) = (A_0 - A_1 + A_0) = (-1 + 4A_0) = \frac{1 + \cos(\pi\omega_l/\omega_0)}{3 - \cos(\pi\omega_l/\omega_0)} \tag{9}$$
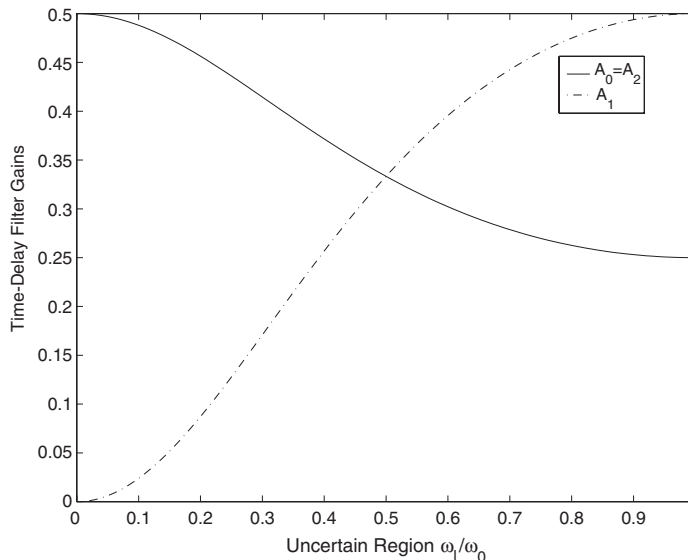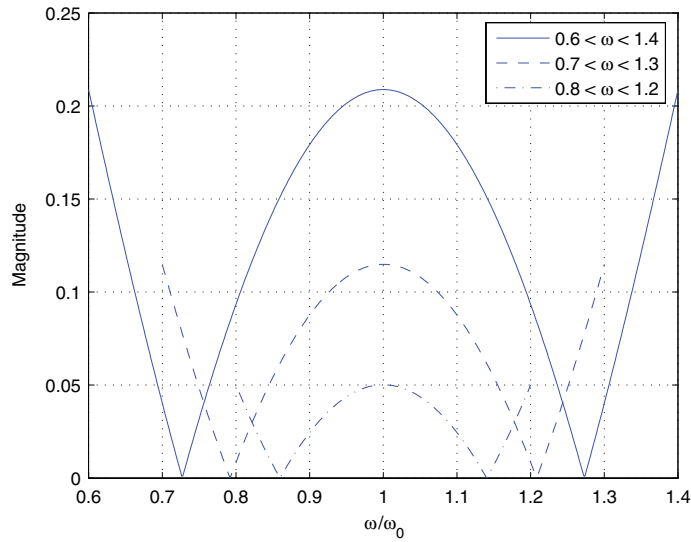

Figure 3. Time-delay filter parameters.

Figure 4. Sensitivity curve.

the uncertain region can be solved given a permissible maximum magnitude of the sensitivity curve. For a given magnitude M, the lower bound of the uncertain frequency range is

$$\omega_l = \frac{\omega_0}{\pi} \cos^{-1}\left(\frac{3M - 1}{M + 1}\right) \tag{10}$$

or the width of the uncertainty is given by the equation

$$2(\omega_0 - \omega_l) = 2\omega_0\left(1 - \frac{1}{\pi}\cos^{-1}\left(\frac{3M - 1}{M + 1}\right)\right) \tag{11}$$

It is also clear from Equation (9) that A_0 lies in the range

$$\tfrac{1}{4} \leqslant A_0 \leqslant \tfrac{1}{2} \quad \Rightarrow \quad 0 \leqslant M \leqslant 1 \tag{12}$$

since the magnitude of the sensitivity curve should not be greater than 1 at the nominal frequency.

The location of zeros of the minimax filter can be solved for by substituting the closed-form solutions for the parameters of the time-delay filter into Equation (1). The equations resulting by equating the real and imaginary parts of Equation (1) to zero lead to

$$A_0 + A_1 \cos(\omega T) + A_2 \cos(2\omega T) = 0 \tag{13}$$

$$A_1 \sin(\omega T) + A_2 \sin(2\omega T) = 0 \tag{14}$$

where $T = \pi/\omega_0$, which have to be solved to determine the locations of the zeros of the time-delay filter. Equation (14) can be rewritten as

$$(1 - 2A_0)\sin(\omega T) + A_0 \sin(2\omega T) = \sin(\omega T)(1 - 2A_0 + 2A_0 \cos(\omega T)) = 0 \tag{15}$$

Table I. Minimax solutions.

Uncertain range	Maximum magnitude $(-1 + 4A_0)$	Zero location $\frac{1}{T}\cos^{-1}\left(\frac{2A_0-1}{2A_0}\right)j$	Zero location $\left(-\frac{1}{T}\cos^{-1}\left(\frac{2A_0-1}{2A_0}\right) + 2\omega_0\right)j$
$0.6 < \omega < 1.4$	0.2088	0.7271j	1.2729j
$0.7 < \omega < 1.3$	0.1149	0.7919j	1.2081j
$0.8 < \omega < 1.2$	0.0501	0.8598j	1.1402j

Table II. Analytical and numerical minimax solutions.

Uncertain range	Numerical optimal cost	Closed-form cost	% Change
$0.6 < \omega < 1.4$	0.20881821054915	0.20881821000003	$-2.63\text{E} - 7$
$0.7 < \omega < 1.3$	0.11489393001650	0.11489393002107	$3.98\text{E} - 9$
$0.8 < \omega < 1.2$	0.05013970954040	0.05013971119400	$3.29\text{E} - 6$

which can be solved resulting in the equation

$$\cos(\omega T) = \frac{2A_0 - 1}{2A_0} \tag{16}$$

which satisfies Equation (13) as well. Thus, the zeros of the time delay filter ($s = \omega j$) are given by

$$\omega = \pm\frac{1}{T}\cos^{-1}\left(\frac{2A_0 - 1}{2A_0}\right) + \frac{2n\pi}{T} = \pm\frac{\omega_0}{\pi}\cos^{-1}\left(\frac{2A_0 - 1}{2A_0}\right) + 2n\omega_0 \tag{17}$$

where n is an integer. Table I lists the location of the zeros and the maximum magnitude of the sensitivity plot as a function of the uncertain range.

The proposed approach is compared to a numerical minimax optimization [11] approach for three uncertain intervals and the results are tabulated in Table II. The minimax problem corresponds to the determination of the parameters of the time-delay filter to minimize the maximum magnitude of the function $F(\omega)$ (Equation (4)). It can be seen that the difference between the numerical and the proposed approach is negligible.

2.2. Non-uniform weighting

To permit differential weighting of the frequencies in the uncertain region, the previous development can be modified to include a penalty at the boundary of the uncertain region. The weight at the nominal frequency is always assumed to be unity. Including the penalty in the formulation results in Equation (6) being modified to

$$W\left(A_0 + A_1\cos\left(\frac{\omega_l}{\omega_0}\pi\right) + A_2\cos\left(\frac{2\omega_l}{\omega_0}\pi\right)\right)^2 + \left(A_1\sin\left(\frac{\omega_l}{\omega_0}\pi\right) + A_2\sin\left(\frac{2\omega_l}{\omega_0}\pi\right)\right)^2$$
$$= (A_0 + A_1\cos(\pi) + A_2\cos(2\pi))^2 \tag{18}$$

For instance, if a gaussian penalty is assumed then

$$W = \exp\left(-\frac{(\omega_l - \omega_0)^2}{2\sigma^2}\right) \tag{19}$$

where σ is the variance of the gaussian distribution. Assuming that $A_2 = A_0$ and therefore $A_1 = 1 - 2A_0$, we can solve Equation (18), resulting in the quadratic equation

$$A_0^2\left(6(W-1) - 8\left(1 + \cos\left(\frac{\omega_l}{\omega_0}\pi\right)\right) - 2\left(1 - \cos\left(\frac{2\omega_l}{\omega_0}\pi\right)\right)\right)$$
$$+ A_0\left(-4(W-1) + 4\left(1 + \cos\left(\frac{\omega_l}{\omega_0}\pi\right)\right)\right) + (W-1) = 0 \tag{20}$$

which can be used to solve for A_0.

Figure 5 illustrates the optimal solutions as a function of different penalties on the boundary and nominal magnitude of the sensitivity curves. It can be seen that as σ decreases, the magnitude of the transfer function of the filter at the nominal frequency also decreases.

2.3. Three time-delay filter

It can be seen from the two time-delay filter that the magnitude of the time-delay filter transfer function at the nominal frequency is non-zero. To force the magnitude at the nominal frequency to zero while minimizing the maximum magnitude of the transfer function over the uncertain domain, a three time-delay filter is proposed as shown in Figure 6.

As in the development for the two time-delay filter, the time delays are assumed to be

$$T_1 = \frac{\pi}{\omega_0}, \quad T_2 = \frac{2\pi}{\omega_0} \quad \text{and} \quad T_3 = \frac{3\pi}{\omega_0} \tag{21}$$
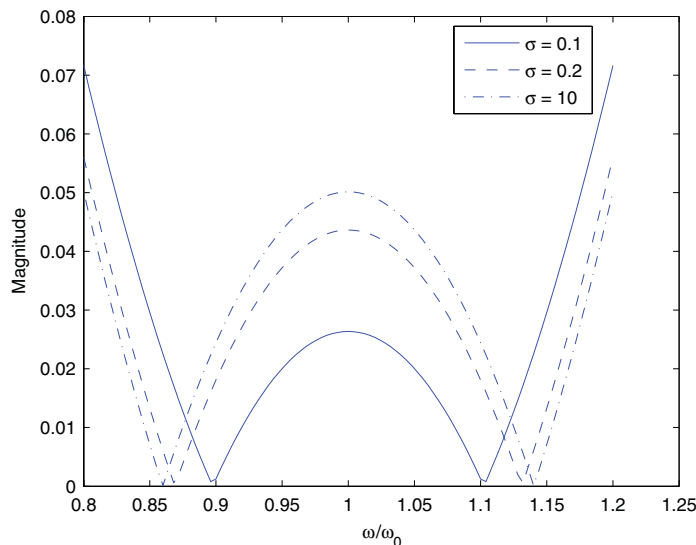

Figure 5. Robust minimax control: varying penalty.

$$r(s) \rightarrow \boxed{A_0 + A_1 e^{-sT_1} + A_2 e^{-sT_2} + A_3 e^{-sT_3}} \rightarrow \boxed{\frac{\omega^2}{s^2 + \omega^2}} \rightarrow y(s)$$
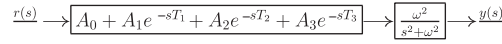
Figure 6. Time-delay filter.

Further, assuming that

$$A_0 = A_3 \quad \text{and} \quad A_1 = A_2 \tag{22}$$

and with the requirement that

$$A_0 + A_1 + A_2 + A_3 = 1 \tag{23}$$

it can be shown that the magnitude of the transfer function of the time-delay filter

$$F(\omega) = 8\cos^3\left(\frac{\omega\pi}{\omega_0}\right)A_0^2 + (4A_0 - 8A_0^2)\cos^2\left(\frac{\omega\pi}{\omega_0}\right) + \left(\frac{1}{2} - 8A_0^2\right)\cos\left(\frac{\omega\pi}{\omega_0}\right) + \frac{1}{2} - 4A_0 + 8A_0^2 \tag{24}$$

is 0 at $\omega = \omega_0$, the nominal frequency. The location of the extremum of the sensitivity curve can be determined from the equation

$$\frac{\mathrm{d}F(\omega)}{\mathrm{d}\omega} = \frac{\pi}{2\omega_0}\left(48A_0^2\cos^2\left(\frac{\omega\pi}{\omega_0}\right) + (16A_0 - 32A_0^2)\cos\left(\frac{\omega\pi}{\omega_0}\right) + 1 - 16A_0^2\right)\sin\left(\frac{\omega\pi}{\omega_0}\right) = 0 \tag{25}$$

Equating the sin term to zero, we have

$$\omega = \omega_0 \tag{26}$$

which corresponds to the minimum at the nominal frequency. The other solution is determined by solving the quadratic equation in the cos term, resulting in

$$\omega = \frac{\omega_0}{\pi}\cos^{-1}\left(\frac{4A_0 - 1}{4A_0}\right) + 2n\omega_0, \quad n = 1, 2, 3\ldots \tag{27}$$

which corresponds to the minimum and

$$\omega = \frac{\omega_0}{\pi}\cos^{-1}\left(-\frac{4A_0 + 1}{12A_0}\right) + 2n\omega_0, \quad n = 1, 2, 3\ldots \tag{28}$$

which corresponds to the maximum. The magnitude of the sensitivity curve at the maximum is

$$F\left(\omega = \frac{\omega_0}{\pi}\cos^{-1}\left(-\frac{4A_0 + 1}{12A_0}\right)\right) = \frac{512A_0^3 - 192A_0^2 + 24A_0 - 1}{54A_0} \tag{29}$$

Equating the magnitude of the transfer function of the time-delay filter at the lower limiting frequency to the maximum, we have

$$8\cos^3\left(\frac{\omega_l\pi}{\omega_0}\right)A_0^2 + (4A_0 - 8A_0^2)\cos^2\left(\frac{\omega_l\pi}{\omega_0}\right) + \left(\frac{1}{2} - 8A_0^2\right)\cos\left(\frac{\omega_l\pi}{\omega_0}\right) + \frac{1}{2} - 4A_0 + 8A_0^2$$

$$= \frac{512A_0^3 - 192A_0^2 + 24A_0 - 1}{54A_0} \tag{30}$$

we can solve the cubic equation for A_0, resulting in the solution

$$A_0 = -\frac{1}{3\cos(\omega_l \pi/\omega_0) - 5}, \quad A_0 = -\frac{1}{4(1 + 3\cos(\omega_l \pi/\omega_0))} \quad \text{and}$$

$$A_0 = -\frac{1}{4(1 + 3\cos(\omega_l \pi/\omega_0))} \tag{31}$$

The second and the third solutions, which are identical, force the boundary to be a maximum resulting in a suboptimal minimax filter. The first solution results in two maxima which lie within the uncertain interval resulting in the optimal minimax solution.

Figure 7 illustrates the variation of the gains of the time-delay filter as a function of the normalized uncertain interval. It can be seen that the amplitudes are always positive as in the two time-delay case. It should be noted that at $\omega_l/\omega_0 = 1$, the solution corresponds to the filter where three identical single time-delay filters, which are designed to cancel the nominal frequency of the system, are cascaded.

Figure 8 illustrates the variation of the sensitivity curve for different uncertain regions. Compared to Figure 4, it can be seen that the maximum magnitude of the three time-delay filter is significantly smaller than the two time-delay filter.

Figure 9 illustrates the variation of the uncertain region as a function of permissible maximum magnitude of the two and three time-delay filter. It is clear that as the maximum permissible magnitude of the time-delay filter, M, is increased, the uncertain region monotonically increases. However, the rate of increase of the uncertain region of the three time-delay filter is large compared to the two time-delay filter in the vicinity of zero permissible magnitude. This implies that for small permissible magnitude, the uncertain region of the three time-delay filter is large.
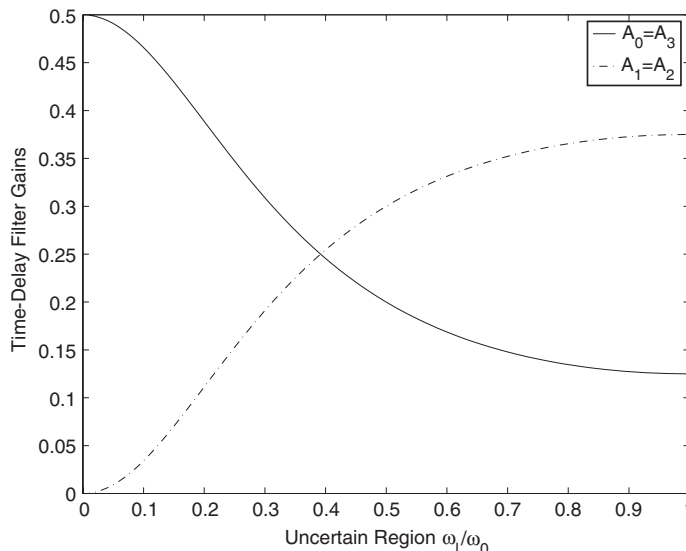

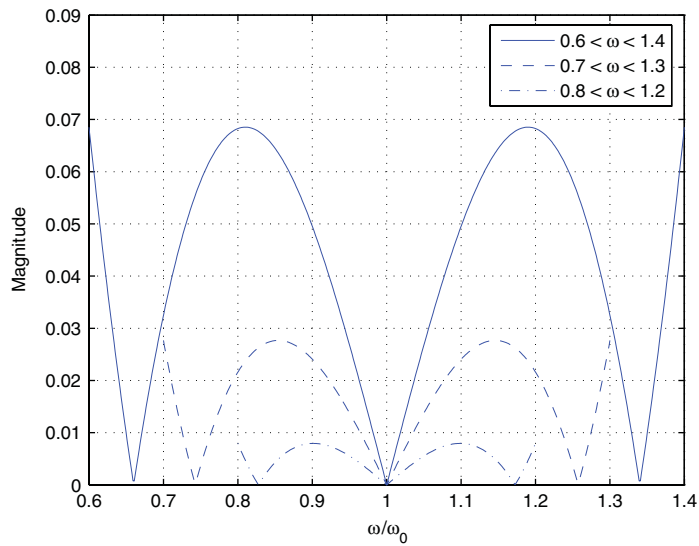
Figure 7. Three time-delay filter parameters.
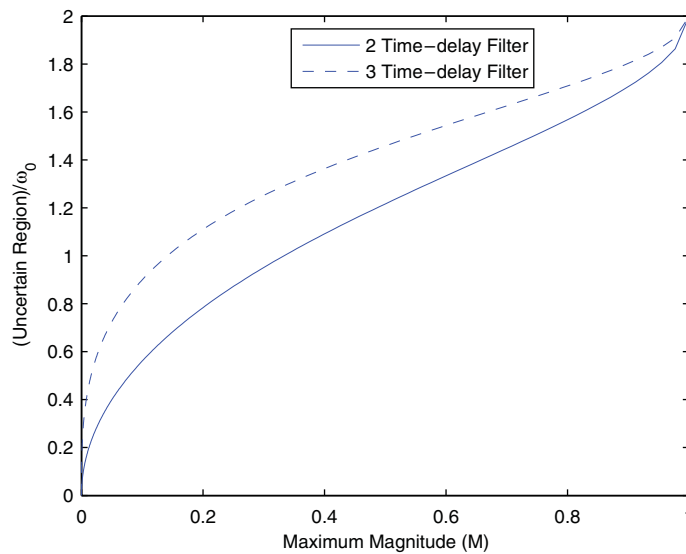
Figure 8. Sensitivity curve.

Figure 9. Uncertain range *vs* permissible magnitude.

3. DAMPED SYSTEMS

To design minimax filters for systems characterized by under-damped behaviour, a simple approach is proposed which uses a transformation to represent the damped system as an

undamped system in the new space. For an under-damped system given by the transfer function

$$G(s) = \frac{\omega^2}{s^2 + 2\zeta\omega s + \omega^2} \tag{32}$$

we define a transformation

$$s = p - \zeta\omega \tag{33}$$

Substituting Equation (33) into Equation (32), we have

$$G(p) = \frac{\omega^2}{p^2 + \omega^2(1 - \zeta^2)} \tag{34}$$

which represents an undamped system with a natural frequency of $\omega\sqrt{1 - \zeta^2}$. The closed-form solution derived earlier for undamped systems can now be used for this transformed system. The time-delay filter can then be transformed back into the original space to arrive at the minimax filter for the damped system.

For instance, the transfer function of a time-delay filter designed to cancel the poles of an undamped system (Equation (34)) is given by the equation

$$F(p) = 1 + \exp\left(-p\frac{\pi}{\omega\sqrt{1 - \zeta^2}}\right) \tag{35}$$

as shown by Singh and Vadali [5]. Transforming this filter into the original space, we have

$$F(s) = 1 + \exp\left(-(s + \zeta\omega)\frac{\pi}{\omega\sqrt{1 - \zeta^2}}\right) \tag{36}$$

which can be rewritten as

$$F(s) = \exp\left(\frac{-\zeta\pi}{\sqrt{1 - \zeta^2}}\right)\left(\exp\left(\frac{\zeta\pi}{\sqrt{1 - \zeta^2}}\right) + \exp\left(-s\frac{\pi}{\omega\sqrt{1 - \zeta^2}}\right)\right) \tag{37}$$

The requirement that the final value of the output of the time-delay filter subject to a unity step input, be unity, requires scaling of the gains of the time-delay filter, resulting in the solution

$$F(s) = \frac{\exp(\zeta\pi/\sqrt{1 - \zeta^2}) + \exp(-s\pi/\omega\sqrt{(1 - \zeta^2)})}{\exp(\zeta\pi/\sqrt{1 - \zeta^2}) + 1} \tag{38}$$

which is identical to the time-delay filter designed to cancel the damped poles as shown by Singh and Vadali [5].

Therefore, the closed-form solution for the gains of the two time-delay minimax filter for a damped system with uncertainty in frequency is given by the equations

$$A_0 = \frac{2(1 + \cos((\omega_l/\omega_0)\pi))}{5 + 4\cos((\omega_l/\omega_0)\pi) - \cos((2\omega_l/\omega_0)\pi)}\exp\left(\frac{2\zeta\pi}{\sqrt{1 - \zeta^2}}\right) \tag{39}$$

$$A_1 = \left(1 - 2\frac{2(1 + \cos((\omega_l/\omega_0)\pi))}{5 + 4\cos((\omega_l/\omega_0)\pi) - \cos((2\omega_l/\omega_0)\pi)}\right)\exp\left(\frac{\zeta\pi}{\sqrt{1 - \zeta^2}}\right) \tag{40}$$

and

$$A_2 = \frac{2(1 + \cos((\omega_l/\omega_0)\pi))}{5 + 4\cos((\omega_l/\omega_0)\pi) - \cos((2\omega_l/\omega_0)\pi)} \tag{41}$$

and the delay times are

$$T_1 = \frac{\pi}{\omega_0\sqrt{1-\zeta^2}} \quad \text{and} \quad T_2 = \frac{2\pi}{\omega_0\sqrt{1-\zeta^2}} \tag{42}$$

and the parameters of the three time-delay minimax filter for a damped system are given by the equations

$$A_0 = \frac{1}{5 - 3\cos(\omega_l\pi/\omega_0)} \exp\left(\frac{3\zeta\pi}{\sqrt{1-\zeta^2}}\right) \tag{43}$$

$$A_1 = \frac{1}{2}\left(1 - 2\frac{1}{5 - 3\cos(\omega_l\pi/\omega_0)}\right)\exp\left(\frac{2\zeta\pi}{\sqrt{1-\zeta^2}}\right) \tag{44}$$

$$A_2 = \frac{1}{2}\left(1 - 2\frac{1}{5 - 3\cos(\omega_l\pi/\omega_0)}\right)\exp\left(\frac{\zeta\pi}{\sqrt{1-\zeta^2}}\right) \tag{45}$$

$$A_3 = \frac{1}{5 - 3\cos(\omega_l\pi/\omega_0)} \tag{46}$$

$$T_1 = \frac{\pi}{\omega_0\sqrt{1-\zeta^2}}, \quad T_2 = \frac{2\pi}{\omega_0\sqrt{1-\zeta^2}} \quad \text{and} \quad T_3 = \frac{3\pi}{\omega_0\sqrt{1-\zeta^2}} \tag{47}$$

The gains A_0, A_1, A_2 and A_3 have to be normalized which is achieved by dividing each of the gains by $A_0 + A_1 + A_2$ for the two time-delay filter case and by $A_0 + A_1 + A_2 + A_3$ for the three time-delay filter case.

Equations (39)–(42) and (43)–(47) are the exact minimax solutions for an uncertain region which lies along the vertical line in the complex plane passing through the nominal damped poles. This implies that both the damping ratio and the natural frequency are varying. The optimal solution when uncertainty exists in the estimated natural frequency implies that the uncertain region is along a straight line passing through the damped nominal pole and the origin. Figure 10 illustrates the difference between the numerical and the closed-form solution for a system with a nominal damping ratio of 0.1 and uncertainty in the natural frequency . The difference between the numerical and closed form increases with increasing uncertainty and it is clear that the difference is not large and occurs at the upper limit of the uncertain region.
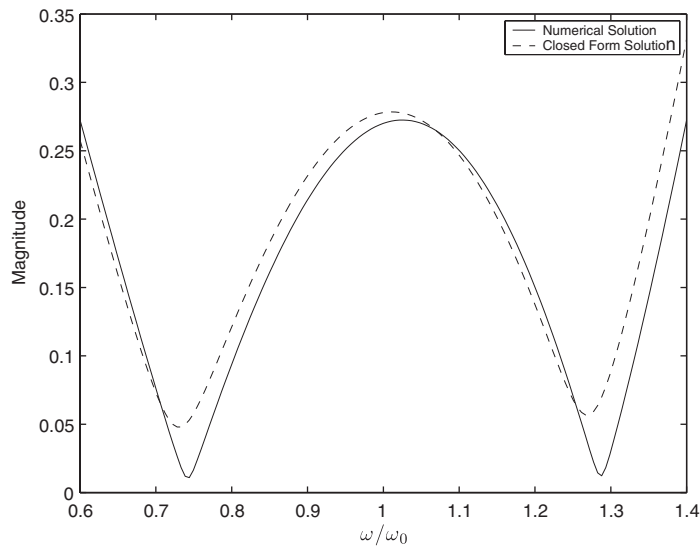
Figure 10. Filter comparison.

4. MULTI-MODE SYSTEMS

The proposed approach can be used to design robust filters for systems whose transfer function includes multiple modes. Time-delay filters are designed for each uncertain frequency and they are subsequently convolved to arrive at a time-delay filter which is robust to all uncertain frequencies.

To illustrate the proposed technique, assume that the two frequencies to be attenuated lie in the range

$$0.8 \leqslant \omega_1 \leqslant 1.2 \quad \text{and} \quad 3.6 \leqslant \omega_2 \leqslant 4.4 \tag{48}$$

and the nominal frequencies are selected to be at the midpoint of the uncertain regions. The transfer functions of the minimax time-delay filters for each of the frequencies are

$$F_1(s) = 0.2625 + 0.4749 \exp(-\pi s) + 0.2625 \exp(-2\pi s) \tag{49}$$

and

$$F_2(s) = 0.2531 + 0.4938 \exp\left(-\frac{\pi}{4} s\right) + 0.2531 \exp\left(-\frac{2\pi}{4} s\right) \tag{50}$$

Figure 11 illustrates the magnitude plot of the minimax filters. The dashed line and the dash-dot lines are the magnitude plots of the filters $F_1(s)$ and $F_2(s)$, respectively. The solid line is the magnitude plot of the final filter which is

$$F(s) = F_1(s)F_2(s) \tag{51}$$

It can be seen that the filter $F(s)$ is robust to uncertainties in both the frequencies.
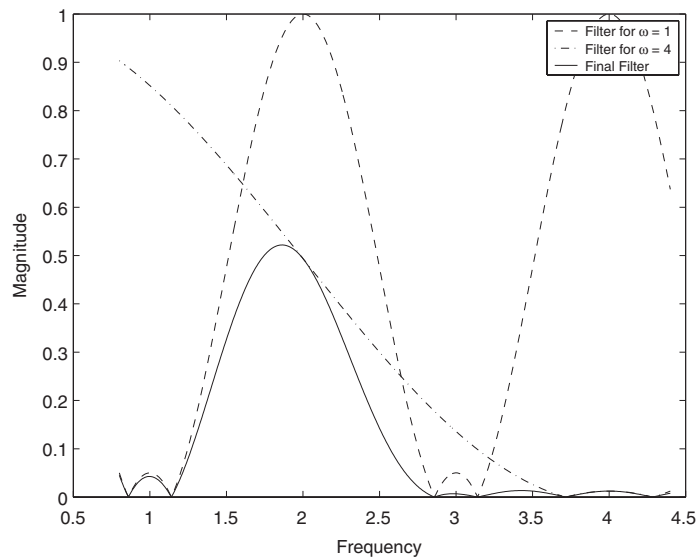
Figure 11. Robust minimax control: multi-mode system.

5. PERFORMANCE ANALYSIS

The proposed technique minimizes the maximum magnitude of the transfer function of a time-delay filter given knowledge of the uncertain domain of the under-damped mode. From a practical viewpoint, the residual energy of the manoeuvring structure is the metric of interest to control designers. It is therefore of interest to determine how the proposed technique for the design of prefilters compares to the minimax filter designed to minimize the maximum residual energy over the uncertain domain, a technique developed by Singh [11]. The residual energy, defined by

$$F = \tfrac{1}{2}\dot{y}^{\mathrm{T}}M\dot{y} + \tfrac{1}{2}y^{\mathrm{T}}Ky \tag{52}$$

where M and K are the mass and stiffness matrices and $\dot{y}$ and y are the velocity and position vectors of the system in consideration, is used to compare the performance of the two filters.

The two time-delay minimax filter which minimizes the maximum magnitude of the residual energy is

$$G(s) = 0.2439 + 0.4554\,\mathrm{e}^{-3.0527s} + 0.3007\,\mathrm{e}^{-2(3.0527)s} \tag{53}$$

and the minimax filter using the closed-form solution proposed in this work is

$$G(s) = 0.2787 + 0.4426\,\mathrm{e}^{-\pi s} + 0.2787\,\mathrm{e}^{-2\pi s} \tag{54}$$

where the uncertain frequency ω lies in the range

$$0.7 \leqslant \omega \leqslant 1.3 \tag{55}$$

It can be seen that the time-delay of the filter which minimizes the residual energy is smaller compared to that of the closed-form solution. To compare the performance of the minimax
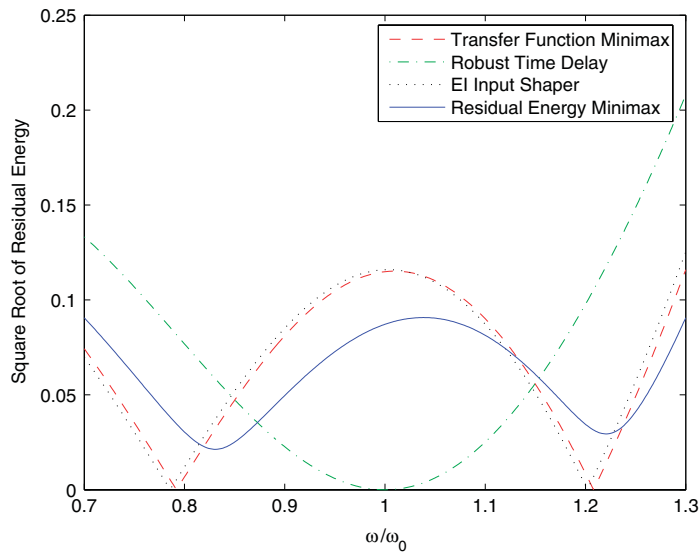
Figure 12. Filter performance: 2 time-delay filter.

filters to the ZVD [10] input shaper which has the same number of delays , the ZVD shaper is designed and is given by the transfer function

$$G(s) = 0.25 + 0.5\,e^{-\pi s} + 0.25\,e^{-2\pi s} \tag{56}$$

Figure 12 illustrates the variation of the square root of the residual energy over the uncertain frequency for three manifestations of the two time-delay filter. It can be seen that the minimax filter, designed using the residual energy as the cost (solid line), performs better than the proposed filter (dashed line). The two minimax filters are also compared to the ZVD filter (dash-dot line) which is designed to place multiple zeros of the time-delay filter at the nominal location of the uncertain poles of the system and the EI input shaper (dotted line). It is clear that the maximum magnitudes of the minimax filters are significantly smaller than the ZVD filter over the uncertain frequency domain. The proposed minimax filter is also marginally better than the EI input shaper.

The next filter which constrains the residual energy to be zero at the nominal frequency results in the filters

$$G(s) = 0.1474 + 0.3492\,e^{-3.1415s} + 0.3526\,e^{-2(3.1415)s} + 0.1508\,e^{-3(3.1415)s} \tag{57}$$

for the residual energy cost and

$$G(s) = 0.1479 + 0.3521\,e^{-\pi s} + 0.3521\,e^{-2\pi s} + 0.1479\,e^{-3\pi s} \tag{58}$$

for the cost proposed in this work. The transfer function for the ZVDD [10] is

$$G(s) = 0.125 + 0.375\,e^{-\pi s} + 0.375\,e^{-2\pi s} + 0.125\,e^{-3\pi s} \tag{59}$$

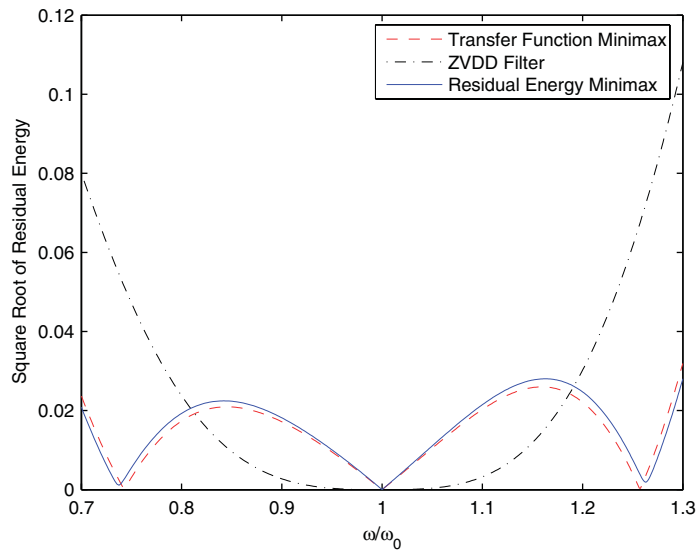which places three sets of zeros of the time-delay filter at the nominal location of the poles of the system.

Figure 13. Filter performance: 3 time-delay filter.

Figure 13 illustrates that the difference between the two minimax filters is not very significant with the proposed prefilter providing a performance which is better than the filter designed to minimize the maximum residual energy, over a large segment of the uncertain range. As in the two time-delay filter, the minimax filters outperform the ZVDD (dash-dot line). The benefit of the proposed technique is that the closed-form solution permits its use in real-time filter design which would be of interest for the design of adaptive filters.

6. CONCLUSIONS

The contribution of this paper is the development of a closed-form solution for the parameters of a time-delay filter which minimizes the maximum magnitude of the transfer function of the time-delay filter. A simple technique to design minimax time-delay filters for underdamped systems is proposed. The minimax two time-delay filter results in non-zero magnitude at the nominal frequency. This magnitude can be reduced by penalizing the magnitude at the nominal frequency compared to the limiting frequencies in the uncertain domain. Closed-form solutions for non-uniform weighting are also derived. Closed-form solutions for the three time-delay filter are also derived which force the magnitude at the nominal frequency to zero.

For systems with non-symmetric uncertain regions around the nominal frequency, the proposed approach can be used by selecting the mean frequency of the uncertain region as the nominal frequency in the design process. The proposed technique can also be used for multi-mode systems by concatenating the minimax filters designed for each uncertain frequency.

ACKNOWLEDGEMENTS

REFERENCES

1. Smith OJM. Posicast control of damped oscillatory systems. *Proceedings of the IRE* 1957; **45**:1249–1255.
2. Singer NC, Seering WP. Preshaping command inputs to reduce system vibrations. *Journal of Dynamic Systems, Measurement and Control* (ASME) 1990; **112**:76–82.
3. Swigert CJ. Shaped torques techniques. *Journal of Guidance and Control* 1980; **3**:460–467.
4. Farrenkopf RL. Optimal open-loop maneuver profiles for flexible spacecraft. *Journal of Guidance and Control* 1979; **2**:491–498.
5. Singh T, Vadali SR. Robust time-delay control of multimode systems. *International Journal of Control* 1995; **62**(6):1319–1339.
6. Junkins JL, Rahman ZH, Bang H. Near-minimum-time maneuvers of distributed parameter systems: analytical and experimental results. *Journal of Guidance, Control and Dynamics* 1991; **14**(2):406–415.
7. Al Mamun A, Ge SS. Precision control of hard disk drives. *IEEE Control System Magazine* 2005; 14–19.
8. Ye X, Yajima N, Ai G, Hu N. Attitude control and high precision pointing control system of a large balloon Borne solar telescope. *Advances in Space Research* 2000; **26**(9):1419–1422.
9. Nelan E, Meixner M, Valenti J, McCullough P. JWST small angle maneuver pointing requirements. *Technical Memorandum*, STSCI-JWST-TM-2003-0015A, Space Telescope Science Institute, September 2003.
10. Singhose W, Porter L, Singer N. Vibration reduction using multi-hump extra-insensitive input shapers. *American Control Conference*, vol. 5, Seattle, WA, 1995; 3830–3834.
11. Singh T. Minimax design of robust controller for flexible systems. *Journal of Guidance, Control and Dynamics* 2002; **25**(5):868–875.
12. Singhose W, Singer N, Seering W. Comparison of command shaping methods for reducing residual vibration. *Proceedings of the 1995 European Control Conference*, vol. 2, Rome, Italy, September 1995; 1126–1131.